An Analytical Bi-Directional Growth Parameterization to Obtain Optimal Castable Topology Designs

Juan Pablo Leiva [*], Brian C. Watson[†] and Iku Kosaka [‡]
Vanderplaats Research & Development, 41700 Gardenbrook, Suite 115, Novi, MI 48375, USA

A new method to produce optimal castable topology designs with optimal parting surfaces is presented. The method is based on parameterizing the design domain and is suitable to be used with gradient-based topology optimization methods. The proposed method takes into consideration irregular meshes commonly used in industrial applications. It also takes into consideration minimum member sizes that are needed for manufacturability and to control the checkerboard phenomena. The method is discipline independent and was tested on linear static and dynamic problems. The method is very efficient as it reduces the number of design variables and does not need to add additional constraints to reflect the manufacturing requirements. The manufacturing requirements are built in a parameterization of the design variables. The development was motivated by the need for generating structural design proposals that could be manufactured with minimum changes. The proposed method was implemented in the GENESIS program and examples that reveal its usefulness are included.

Nomenclature

A^e_i	=	area density of element i
A^g_j	=	area density of grid j
A^p_k	=	area density of pole k
B^e_i	=	height of carved material of the design domain on the vicinity of element i
D_{jk}	=	radial distance between grid j and pole k
ρ^e_i	=	volume fraction of element i
F	=	objective function
g_j	=	jth constraint
h	=	discretization parameter
h^e_i max	=	maximum height of element i
h^e_i min	=	minimum height of element i
H^e_i	=	height of filled material of the design domain on the vicinity of element i
H^e_i max	=	maximum height of the design domain on the vicinity of element i
H^e_i min	=	minimum height of the design domain on the vicinity of element i
i	=	element index
j	=	grid index or constraint index when used with gj
k	=	pole index
l^e_i	=	element growth fraction of element i
L^e_i	=	growth fraction at element i measured from bottom of design domain
L^g_j	=	growth fraction at grid j measured from bottom of design domain
L^p_k	=	growth fraction at pole k measured from bottom of design domain
c^e_i	=	element carve fraction of element i
C^e_i	=	carve fraction at element i measured from bottom of design domain
C^g_j	=	carve fraction at grid j measured from bottom of design domain

[*] Genesis Project Manager, jp@vrand.com, Senior Member AIAA.
[†] Senior Engineer, bwatson@vrand.com, Senior Member AIAA.
[‡] Senior R&D Engineer, ikosaka@vrand.com.

C^p_k = carve fraction at pole k measured from bottom of design domain
W_{jk} = weighting factor jk
Ω = design domain
Ω_{xy} = parametric design domain

I. Introduction

The field of manufacturing engineering has been developed for hundred of years. Today several methods such as casting, forming, molding and machining are available to shape metals into final products or components. It is interesting to mention here that objects such as copper arrowheads and ornaments were made 6000 years ago using casting[1]. Many casting processes have been developed over the years and their manifestation can be found in many of the products we use in our daily lives. The design of many of these objects has been done over the years based on judgment, experience or history. Structural analysis to study the behavior of part has only been used in the last few decades. Optimization has been used even less. However, intense competition started to change that and now optimization is starting to be used more and more. In the last decade, topology optimization has started to show its usefulness to find innovative designs that increase the performance of the products designed with it. This intense competition in the market place has forced software vendors to add topology optimization into their products and more recently, forced them to refine its capability to take into consideration more and more specific issues related to manufacturing.

The field of topology optimization has rapidly developed since it was first introduced in the late eighties[2]. However, little work has been done to take in consideration manufacturing requirements such as avoiding the formation of interior cavities. Consequently, designers using topology optimization have encountered difficulties interpreting results and adapting them to their final designs. This motivated us to study how to add this capability to the GENESIS[3] program. In researching the literature, only few papers can be found that deal with this subject. Harzheim and co-workers, from Adams Opel AG, introduced methods that attempt to incorporate casting requirement in topology optimization[4]. They developed a “biological” growth rule based on stress levels in a prescribed direction and added it on the TopShape program. Their implementation seems to work well for this task. However, since the “biological” growth rule is not based on a differentiable analytical expression, it is not usable for programs like GENESIS, that require gradient information to perform optimization. Another drawback of the biological rule implemented in TopShape is that it requires the finite element model to use a voxel mesh (regular mesh build with hexahedral elements). Zhou and co-workers, proposed an alternative method for optimizing parts with casting requirements. Their proposed method is suitable for non-linear programming based topology optimization programs[5]. Their approach consists of creating a series of constraints that essentially forces the densities of element in “lower” rows to be higher than the densities of elements in “higher” rows. In other words, their approach creates mathematical constraints to enforce the manufacturing requirements. This approach seems to be unnecessary expense as it introduces too many new constraints on the design variables.

In a recent publication[6], we introduced a new method to produce castable topology designs, termed the Analytical Directional Growth Parameterization (ADGP). This method is currently implemented in GENESIS, and has the following characteristics:

- Discipline independent
- Works with regular or irregular meshes.
- Efficient: It reduces the design variable without increasing the number of constraints.

The ADGP method works by parameterizing the design variables of the design domain. However, the ADGP method had a limitation that required that the parting surface be at a fixed, predefined location: the bottom or the top of the designable region. A variable parting surface is important in many designs, so a challenge remained to be solved. It should be noted here that this limitation does not exist in the method described in Ref. 4. In this paper we present a new method that improves the ADGP method by adding new variables to allow for having a variable parting surface. The new method, as it will be shown later in this paper, generalizes the ADGP method and retains the main characteristics listed above. It should be mentioned here that having a fixed parting surface is not always a limitation, so the ADGP equation is still useful.

II. The Optimization Problem

The topology optimization problem of interest is expressed as:

$$\begin{aligned}
&Min\, F(\rho_1, \rho_2, \ldots, \rho_n) \\
&\text{such that :} \\
&g_j(\rho_1, \rho_2, \ldots, \rho_n) \le 0; \quad j = 1, m \\
&0.0 \le \rho_i \le 1.0; \quad i = 1, n
\end{aligned} \tag{1}$$

where F is the objective function, g_j are the constraints and ρ_i are the design variables that represents element volume fractions

This topology optimization problem is solved in GENESIS using a sequence of approximate problems based on the approximation concept approach. Each approximate problem contains approximate functions and is solved using the general-purpose optimizer BIGDOT. The material properties are updated using predefined rules (Power, Reuss, Voigt and/or combination of the last two) that help to get 0-1 solutions that represent the void or solid state of each of the designable elements in the finite element model.

In the mid-seventies[7-8], Schmit et al. introduced approximation concepts for traditional structural optimization. In the mid-eighties[9-16] efficient ways to approximate functions has been developed. The idea to design a Young's modulus with a predefined rule for the purpose of creating voids that represent a topological design was presented by Bendsoe et al. in the late eighties[17]. The Reuss and Voigt rules are discussed in Ref. 18. The BIGDOT program is a large-scale, non-linear, exterior-penalty based optimizer developed by Vanderplaats[19]. Details on how these key ideas and others are implemented in the GENESIS program can be found in Ref. 20.

III. Design Variables

As topology optimization is used to solve for the material distribution problem, the traditional approach has been to select the element volume fractions as the design variables. The element volume fraction is defined as follows:

$$\rho_i = \frac{V_i^e}{V0_i^e} \tag{2}$$

where V_i^e is the solid fraction of volume in the element i and $V0_i^e$ is the total volume of element i.

IV. The Growth Direction

The growth direction is the direction where the structure will be allowed to grow. The arrow pointing upward on the right of the U shape structure in Fig. 1 represents a pre-selected growth direction with a parting surface located at the bottom of the design domain. The double head arrow in the right of the H shaped structure represents a growth direction without a fix-parting surface. The left part of Fig. 1 shows the hypothetical initial design of a structure before optimization. The gray color indicates it has a uniform distributed material that is neither fully solid nor fully void. The second structure from the left shows a typical topology optimization result that maximizes the stiffness of

Figure 1. The Growth Direction

the structure, subject to a torsional load. The black color denotes a fully solid state and the white in the center a fully developed hole. The two structures on the right of Fig. 1 shows two desirable topology result for casting, they are not an optimum from the stiffness point of view, but they can be manufactured with a casting process. The U shaped section has its parting surface on the bottom. The H shaped section has a variable parting surface.

V. Design Variable Parameterization

The key idea of this work is to parameterize the element volume fractions with parameters that explicitly take into consideration the growth direction. The relationship between the element volume fraction and the elements parameters is shown next:

$$\rho_i^e = A_i^e * l_i^e * c_i^e \tag{3}$$

where A_i^e is the element area density , l_i^e is the element growth fraction and c_i^e is the element carve fraction.

The element area density is the density of the element when it is completely filled. The product $l_i^e * c_i^e$ measures if the element is completely filled with material ($l_i^e * c_i^e$ =1.0), is partially filled with material (0.0< $l_i^e * c_i^e$ <1.0 or not filled at all ($l_i^e * c_i^e$ = 0). The element growth fractions and carve fractions are parallel to the die direction.

A. Pole Parameters

A coordinate system that has its z-axis parallel to the growth direction is used. All grids are transformed to that coordinate system to simplify calculations. A plane that is perpendicular to z is used as a reference plane. The projection of the design domain Ω into the XY plane is defined as the parametric domain Ω_{xy}, which is discretized using a constant spacing h. Lines parallel to the growth direction that start on the discrete points of Ω_{xy} are named poles. The total number of poles is NP.

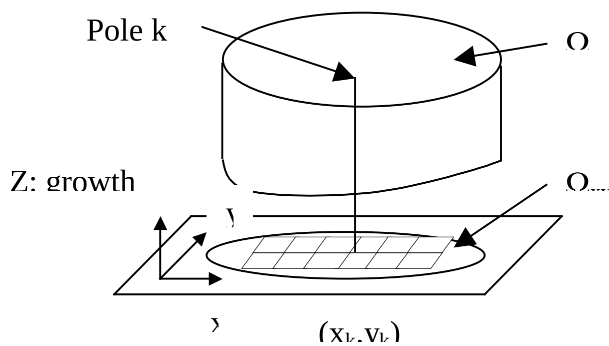

Figure 2. The Pole Parameters

For every pole in Ω_{xy}, three parameters are used: A_k^p, L_k^p and C_k^p. The first parameter is named pole area density and is constructed to represent the density in the vicinity of the pole *k*. The second parameter, L_k^p, is named pole growth fraction and represents the fraction of the height in the vicinity of pole *k* that is filled with material. The third parameter, C_k^p, is named pole carve fraction and represents the fraction of the height in the vicinity of pole *k* that is carved from the bottom.

The pole area density, the pole growth fraction and the pole carve fraction parameters can take values between 0.0 and 1.0.

$$\left.\begin{array}{l} 0.0 \le A_k^p \le 1.0 \\ 0.0 \le L_k^p \le 1.0 \\ 0.0 \le C_k^p \le 1.0 \end{array}\right\} \tag{4}$$

For convenience the parameters can be stored as vectors:

$$
\begin{aligned}
\vec{A} &= (A_1^p, A_2^p, .., A_{NP}^p) \\
\vec{L} &= (L_1^p, L_2^p, ..., L_{NP}^p) \\
\vec{C} &= (C_1^p, C_2^p, ..., C_{NP}^p)
\end{aligned}
\tag{5}
$$

B. Grid Parameters

The area densities, the growth fraction and carve fraction parameters are calculated at the grids as weighted averages of their corresponding pole parameters as shown next:

$$
\left.
\begin{aligned}
A_j^g &= \sum_{k=1}^{NPj} w_{jk}(x_j, y_j) A_k^p \\
L_j^g &= \sum_{k=1}^{NPj} {}^* w_{jk}(x_j, y_j) L_k^p \\
C_j^g &= \sum_{k=1}^{NPj} {}^* w_{jk}(x_j, y_j) C_k^p
\end{aligned}
\right\}
\tag{6}
$$

Where:

$$
w_{jk}(x_j, y_j) = \frac{e^{-\alpha\left(\frac{D_{jk}}{s}\right)^2}}{\sum_{k=1}^{NPj} e^{-\alpha\left(\frac{D_{jk}}{s}\right)^2}}
\tag{7}
$$

$$
D_{jk}(x_j, y_j) = \sqrt{(x_j - x_k)^2 + (y_j - y_k)^2}
\tag{8}
$$

In the above equations w_{jk} is a Gaussian weighting factor similar to the ones used in meshless methods[21]. The weighting factors are normalized so that when all pole parameters are 1.0, the corresponding grid parameters are 1.0. In the exponential expression, s and α are predefined values used to accelerate or reduce the influence of the pole on the grids; s and α, along with the h parameter, are also used to impose a minimum member size. D_{jk} is the radial distance from grid j to pole k. As these expressions are z independent, they essentially enforce a constant function value over z. It should be noticed that the weighting factors with small values are discarded and that the equations associated to them are restricted to work only with the relevant weighting factors.

C. Element Parameters

The area density and the growth fraction evaluated at the center of the element i can be calculated as a simple average of the grids that define the element:

$$
\left.
\begin{aligned}
A_i^e &= \sum_{j=1}^{NGi} \frac{A_j^g}{NGi} \\
L_i^e &= \sum_{j=1}^{NGi} \frac{L_j^g}{NGi} \\
C_i^e &= \sum_{j=1}^{NGi} \frac{C_j^g}{NGi}
\end{aligned}
\right\}
\tag{9}
$$

NGi is the number of the grids associated with ith element. This averaging is intended to help to get a better approximation at the center of the element on coarse meshes. An alternative and simpler scheme would be to evaluate these parameters at the center of the element. Working with grid parameters also helps to use the method with irregular meshes with non-uniform elements.

D. Interpolation Functions

Combining Eqs. (6) and (9) gives the following interpolation functions:

$$\left.\begin{array}{l} A_i^e = \Psi_i\left(\vec{A}\right) \\ L_i^e = \Psi_i\left(\vec{L}\right) \\ C_i^e = \Psi_i\left(\vec{C}\right) \end{array}\right\} \tag{10}$$

Where

$$\left.\begin{array}{l} \Psi_i\ (\vec{A}) = \sum_{j=1}^{NGi} \frac{1}{NGi}(\sum_{k=1}^{NP} W_{jk}(x_j, y_j) A_k^p) \\ \Psi_i\ (\vec{L}) = \sum_{j=1}^{NGi} \frac{1}{NGi}(\sum_{k=1}^{NP} W_{jk}(x_j, y_j) L_k^p) \\ \Psi_i\ (\vec{C}) = \sum_{j=1}^{NGi} \frac{1}{NGi}(\sum_{k=1}^{NP} W_{jk}(x_j, y_j) C_k^p \end{array}\right\} \tag{11}$$

E. Analytical Growth Rule

Having calculated the growth fraction L^e_i on the vicinity of the element *i*, one can calculate the actual material growth on the vicinity of the element i in length units:

$$H_i^e(L_i^e) = (H_i^e \max - H_i^e \min) * L_i^e + H_i^e \min \tag{12}$$

In the preceding equation, $H_i^e \max$ and $H_i^e \min$ correspond to characteristic maximum and minimum heights of the design domain in the vicinity of the element *i*. See Figure 3 for a detail description of these dimensions.

From the actual material growth one can calculate the element growth fraction using the following expression:

$$l_i^e = \Phi(H_i^e) = \begin{cases} \phi(H_i^e) & \text{if } h_i^e \min \le H_i^e \le h_i^e \max \\ 1.0 & H_i^e \ge h_i^e \max \\ 0.0 & H_i^e \le h_i^e \min \end{cases} \tag{13}$$

Where:

$$\phi\ (H_i^e) = \frac{H_i^e - h_i^e \min}{h_i^e \max - h_i^e \min} \tag{14}$$

In the preceding equation, h^e_i max is the maximum height of element *i* and h^e_i min is the minimum height of that element.

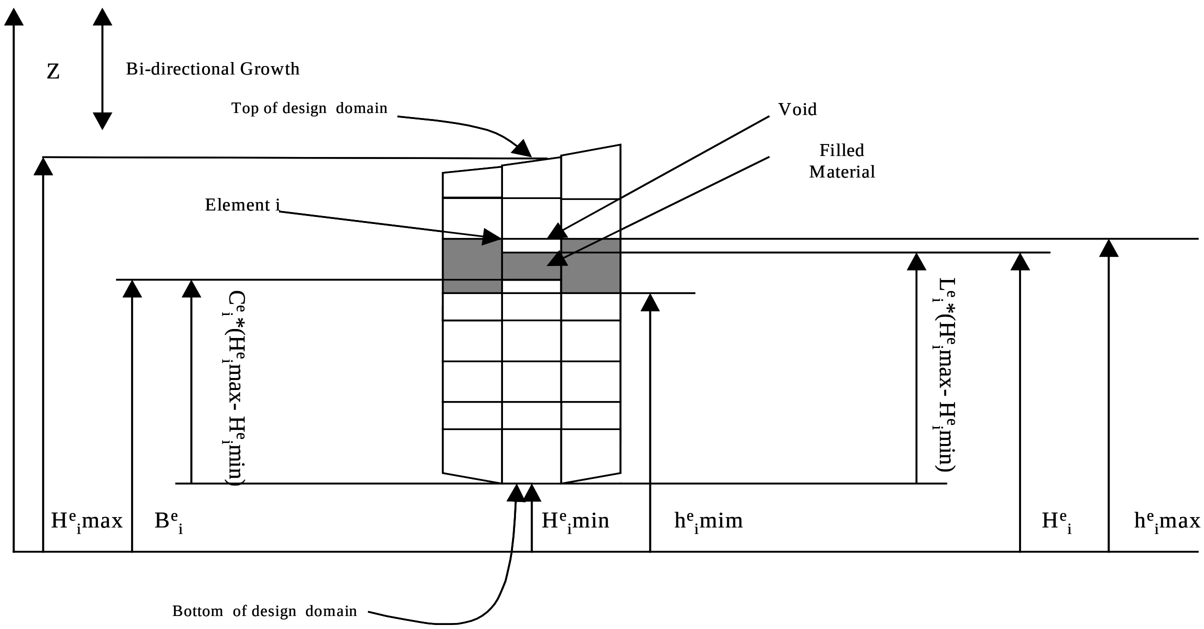

Figure 3. The Growth and Carve Parameters

By combining Eqs. (10), (12), and (13), we can construct an equation that links the pole growth fraction with the element growth fraction:

$$\ell_i^e = \Phi_i \left(H_i^e \left(\Psi_i \left(\vec{L}\right)\right)\right) \tag{15}$$

or

$$\ell_i^e = \ell_i^e \left(H_i^e \left(L_i^e \left(\vec{L}\right)\right)\right) \tag{16}$$

Having calculated the carve fraction C^e_i measured at the element *i*, one can calculate the actual material carved in length units:

$$B_i^e(C_i^e) = (H_i^e \max - H_i^e \min) * C_i^e + H_i^e \min \tag{17}$$

From the carved material the element carve fraction can be calculated using the following expression:

$$c_i^e = \Phi'(B_i^e) = \begin{cases} 1.0 - \phi(B_i^e) & \text{if } h_i^e \min \le B_i^e \le h_i^e \max \\ 0.0 & B_i^e \ge h_i^e \max \\ 1.0 & B_i^e \le h_i^e \min \end{cases} \tag{18}$$

Where:

$$\phi(B_i^e) = \frac{B_i^e - h_i^e \min}{h_i^e \max - h_i^e \min} \tag{19}$$

Comparing Eqs. (13) and (18) we can obtain:

$$c_i^e = 1.0 - \Phi(B_i^e) \quad \textbf{(20)}$$

By combining Eqs. (10), (17) and (20), we can construct an equation that links the pole carve fraction with the element carve fraction:

$$c_i^e = 1.0 - \Phi_i\,(B_i^e(\Psi_i\,(\vec{C}))) \quad \textbf{(21)}$$

or

$$c_i^e = 1.0 - c_i^e(B_i^e(C_i^e(\vec{C}))) \quad \textbf{(22)}$$

Multiplying Eqs. (15) and (22) we can construct the following growth rule:

$$b_i^e = l_i^e * c_i^e = \Phi_i\,(H_i^e(\Psi_i\,(\vec{L}))) * (1.0 - \Phi_i\,(B_i^e(\Psi_i\,(\vec{C})))) \quad \textbf{(23)}$$

The product of Equations $b^e{}_i$ = $l_i^e * c_i^e$ represents a rule for filling or emptying the element bi-linearly. This approximation could be replaced with a more accurate one, but we consider that it is good enough, as its only purpose is to achieve a 0-1 solution where it is sufficient to know if the element is completed filled or not. This growth rule is an explicit function of the pole parametric variables. This rule provides a way to analytically describe the filling and carving of material.

VI. Analytical Bi-Directional Growth Parameterization

Combining Eqs. (3), (10), (15) and (22) yields the following equation:

$$\rho_i^e = \rho_i^e(\vec{A},\vec{L},\vec{C}) = \Psi_i^e(\vec{A}) * \Phi_i^e(H_i^e(\Psi_i^e(\vec{L}))) * (1.0 - \Phi_i^e(B_i^e(\Psi_i^e(\vec{C})))) \quad \textbf{(24)}$$

Equation (24) gives an explicit relationship between the pole parameters and the element volume fraction. This equation is differentiable with respect to the pole parameters and is termed here the "Analytical Bi-Directional Growth Parameterization" (ABDGP) equation.

A. Casting Designs with variable parting planes

To generate designs that are suitable for casting where the parting plane is not fixed the ABDGP equation can be used directly by picking the appropriate growth direction. In this case, the topology optimization problem is modified as follow:

$$\begin{aligned}
&\text{Min } F(\rho_1, \rho_2, \ldots, \rho_n) \\
&\text{such that:} \\
&g_j(\rho_1, \rho_2, \ldots, \rho_n) \le 0; \quad j = 1, m \\
&\rho_i = \rho_i\,(\vec{A},\vec{L},\vec{C}) = \Psi_i^e(\vec{A}) * \Phi_i^e(H_i^e(\Psi_i^e(\vec{L}))) * (1.0 - \Phi_i^e(B_i^e(\Psi_i^e(\vec{C})))); \quad i = 1, n \\
&0.0 \le A_k^p, L_k^p, C_k^p \le 1.0; \quad k = 1, NP
\end{aligned} \quad \textbf{(25)}$$

This problem is essentially the same as the one described in (1), as it considers the same objective function and the same constraints. However, the densities now are restricted to change with the pole parameters. The pole parameters become the independent design variables. When the optimization problem needs to evaluate the *F* or *g* functions, the ABDGP equation is used to calculate the needed densities.

The initial values of the pole parameter should be 1.0 for L^p_k, 0.0 for C^p_k and the desired mass fraction for A^p_k.

It is interesting to mention here that this parametric topology optimization problem uses far fewer design variables than the original. The actual number of parameters depends on the pre-selected discretization parameter *h*. If *h* is picked to be the average size of an element, the reduction in the number of design variables is dramatically high. For example for a cube of 100*100*100 elements the number of pole design variables is 3*100*100, that is, 33 times smaller. This should not be surprising as the parameterization is essentially solving a 3D problem via a projection to 2D.

B. Casting Designs with a Fix Parting Surface on the Bottom of the Design Domain

By fixing the carve design variables C_k^p variables to 0.0 we can produce design proposal that have a fixed parting surface on the bottom of the design domain. This is also equivalent to use only the pole area densities parameters and the pole growth fractions. In this case the reduced ABDGP equation produces the following optimization problem:

$$\begin{aligned}
&\text{Min } F(\rho_1, \rho_2, \ldots, \rho_n) \\
&\text{such that:} \\
&g_j(\rho_1, \rho_2, \ldots, \rho_n) \le 0; \quad j = 1, m \\
&\rho_i = \rho_i(\vec{A}, \vec{L}) = \Psi_i^e(\vec{A}) * \Phi_i^e(H_i^e(\Psi_i^e(\vec{L}))); \quad i = 1, n \\
&0.0 \le A_k^p, L_k^p \le 1.0; \quad k = 1, NP
\end{aligned} \qquad \textbf{(26)}$$

This reduced optimization problem is identical to the one we presented in Ref. 5. In there, the parametric equations that produced this formulation are termed ADGP. In other words, the ABDGP equation reduces to the ADGP equation. This reduced parametric topology optimization problem uses 2*NP independent design variable, this is one third less the number design variables used by the ABDGP equations.

C. Extrusion Designs

To obtain designs that represent extrusions, the ABDGP equation is simplified by fixing simultaneously the L_k^p variables to 1.0 and the C_k^p variables to 0.0. This is also equivalent to only use the pole area densities parameters. In this case the reduced ABDGP equation is:

$$\rho_i = \rho(\vec{A}) = \Psi_i(\vec{A}) \qquad \textbf{(27)}$$

In this case the topology optimization problem is modified as follow:

$$\begin{aligned}
&\text{Min } F(\rho_1, \rho_2, \ldots, \rho_n) \\
&\text{such that:} \\
&g_j(\rho_1, \rho_2, \ldots, \rho_n) \le 0; \quad j = 1, m \\
&\rho_i = \rho_i(\vec{A}) = \Psi_i(\vec{A}); \quad i = 1, n \\
&0.0 \le A_k^p \le 1.0; \quad k = 1, NP
\end{aligned} \qquad \textbf{(28)}$$

This reduced parametric topology optimization problem uses NP independent design variable, one third of the number of design variables used by the parametric topology optimization problem proposed for casting designs with variable parting surface and one half the number of variables used for the parametric topology optimization problem with fixed parting plane.

VII. Minimum Member Size

Minimum member size controls are used to obtain topology design proposals without thin members. The equation presented here can be used to control minimum member size. Figure 4 shows the effect of using different values of the pole spacing parameter *h*. The same problem with same finite element mesh was solved using 3 different values of *h*.

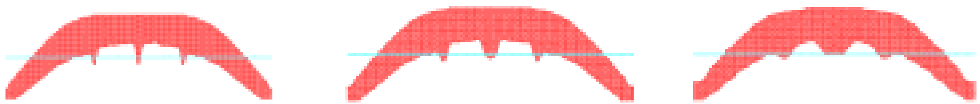

Figure 4. Casting Optimization Results with Different Minimum Member Sizes

VIII. Numerical Applications

A. 3-D Space Truss

Description of the Problem

This problem consists of finding the optimal location of material to support a vertical load applied on the middle bottom part of the block shown in Figure 5a. The structure is supported on each of its four bottom corners. The exterior dimensions of the block are 20x20x10 mm^3. The block is modeled with a 20x20x10 mesh consisting of 4000 hexahedral elements, 4,851 grids and 14,546 degrees of freedoms. The optimization problem is defined to minimize the global strain energy while keeping 25% of the material. Four cases are used to compare the design proposals that results from ignoring casting manufacturing constraints or imposing them in three alternative directions.

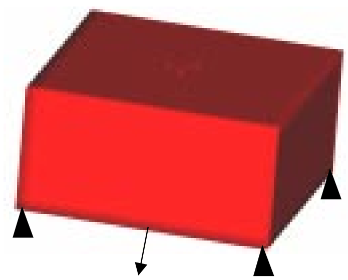

Figure 5a. Designable Region

Figure 5b. Standard Topology Results

Results

In the first case a standard topology optimization was performed using 4000 independent design variables. Figure 5b shows the topology results. In this figure interior holes are revealed. This result is not possible to manufacture with a simple casting. In the other three cases, the ABDGP equations were used to find design proposal suitable for casting. Tree different directions are used. In the first and second cases 600 independent design variables were used. Figures 6 show the results. Due to symmetry these two answers are identical. In the fourth case, 1200 design variables were used. Fig. 6 also shows these results.

Figure 6: Casting Topology Results

B. Beam Design

Description of The Problem

This problem is used in Ref. 22 to test the capability of the BIGDOT optimizer to solve problems with a large number of design variables. Here we use it to demonstrate the ABDGP equation and it usability for handling models with four node tetrahedral elements. The problem consists of finding the optimal location of material to support a vertical load applied on the central part of the bottom of the beam. The beam is supported by single point constraints in its four bottom corners. The exterior dimensions of the block are 56x20x10. The finite element mesh used in this problem contains 1,003,520 four node tetrahedral elements and 188,033 grids. The total number of degrees of freedom is 564,147. The optimization problem consists of minimizing the global strain energy while keeping 10% of the material.

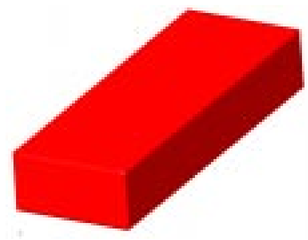

Figure 7. Design Space

Results

In the first case, a standard topology optimization was performed using 1,003520 independent design variables, i.e., one design variable per designable element. The optimization process took 20 design cycles to complete. Figure 8 shows different views of the topology results. The obtained design proposal looks reasonable as the load can be carried from its point of application to the four corners of the structure.

In the second case the ABDGP method is used to find a design proposal suitable for casting. The selected growth

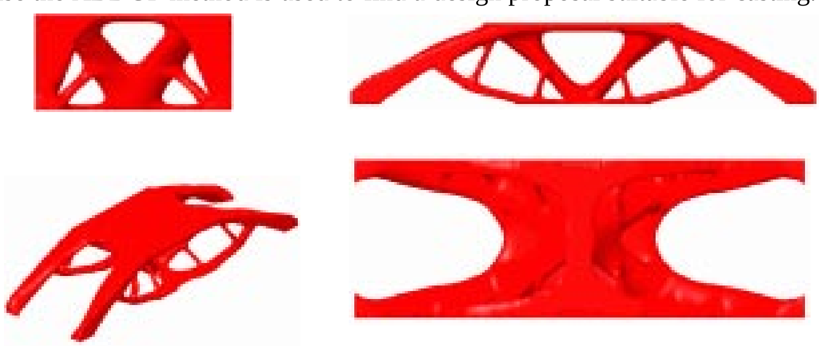

Figure 8. Different Views of Standard Topology Results

direction coincides with the z direction. The two arrows pointing in opposite directions in Figure 9 show the bi-directional growth direction. In total, 13,440 (4480*3) independent design variables were used. In other words, the number of variable used is 98.66% less than the number of variables used on the first case. In this case the optimization process took 19 design cycles to complete. The final results show that the structure does not have interior holes, as desired; so it can be manufactured using a casting process.

Figure 9. Topology Results for Casting in the Z Direction

In the third case the ABDGP method is also used to find a design proposal suitable for casting. In this case, the selected growth direction coincides with the x direction. The two arrows pointing in opposite directions in Figure 10 show the bi-directional growth direction. In this case only 6,720 (2240 poles) independent design variables were used. In this case the optimization process took 22 design cycles to complete. Figure 10 also shows the topology results. The final results show that the structure does not have interior holes, as desired; so it can also be manufactured using a casting process as on the previous case.

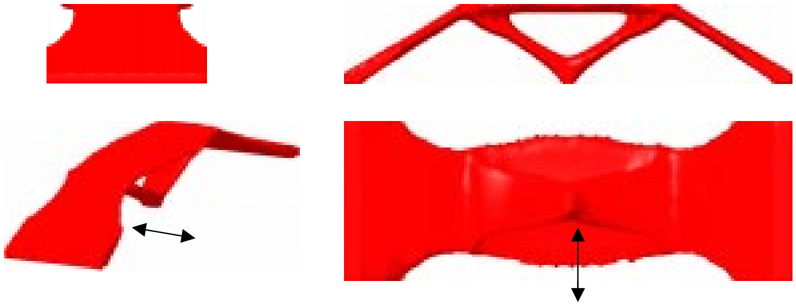

Figure 10. Topology Results for Casting in the X Direction

In the fourth case the ABDGP method is also used to find a design proposal suitable for casting. In this case, the selected growth direction coincides with the y direction. The arrows pointing in opposite directions in Fig. 11 shows the bi-directional growth direction. In this case only 2,400 (800*3) independent design variables were used. In other words, the number of variable used is 99.76% less than the number of variables used on the first case. In this case the optimization process took 22 design cycles to complete. Figure 11 also shows the topology results. The final results show that the structure does not have interior holes and it can be manufactured using a casting process.

Figure 11. Topology Results for Casting in the Y Direction

C. Bridge Design I

Description of the Problem

The following example is used to demonstrate the effectiveness of the ABDGP method. The problem consist on finding the optimal distribution of material that will minimizing the global strain energy while keeping up to 30% of the material. The problem consists of finding the support of the two dimensional bridge. The dimensions of the bridge are 120 m. by 40 m. The structure is fixed in the two lower corners and loaded with a five point loads separated by 20 m. each. The model contains 37,920 designable triangular elements and 480 non-designable ones that model the road. Three cases are used to compare the design proposals that results from ignoring manufacturing requirements or imposing them.

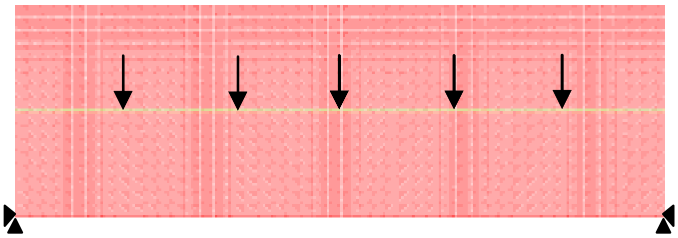

Figure 12: Initial Design and Load Condition

Results

In the first case, standard topology optimization was performed. In this case 37,920 independent design variables were used. In the second case the ABDGP method was used considering a vertical bi directional growth direction. In total 1,440 independent design variables were used. The results in Figure 13 show that the structure does not have interior holes so this structure can be manufactured using a casting process. In the third case the ADGP method was used to study results where the parting plane is fixed in the bottom. In this case 960 independent design variables were used.

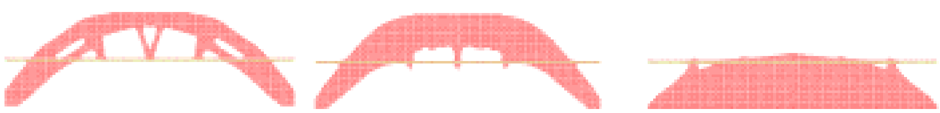

Figure 13. Topology Results with Triangular Elements: *Standard, Casting with variable parting Surface and Casting With Fix Parting Surface on Bottom*

D. Bridge Design II

To verify the answers obtainied with the triangular mesh, the same problem was solved with a mesh assembled with 19,200 quadrilateral elements. The results are shown in Figure 14. These results are similar to the one obtained with the previous mesh. This verify that the method works well with the triangular mesh.

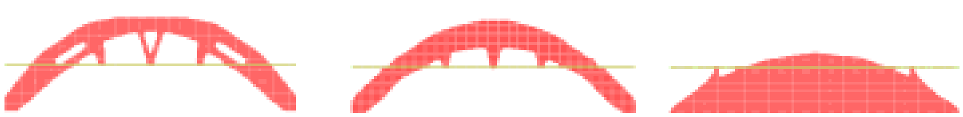

Figure 14. Topology Results with Quadrilateral Elements: *Standard, Casting with variable parting Surface and Casting With Fix Parting Surface on Bottom*

IX. Conclusions

An analytical bi-directional directional growth equation for parameterzing the design variable space to produce castable topology design proposals has been presented. The method allows for controlling minimum sizes that are also important for manufacturing. Numerically the method avoids mesh dependencies and controls the checkerboard phenomena. The method is suitable to be used with optimization programs based on mathematical nonlinear programming optimization. The method improves and provides and alternative to the ADGP method that requires a fixed parting surface. The method presented here is more efficient than other alternative methods since it uses fewer design variables and does not need to deal directly with mathematical constraints that simulate the manufacturing requirement.

Although the presented method was originally developed to be used with 3D structures, it can be used in 2D structures as well. If the growth direction is contained in the plane of the structure then the method can be used to design planar castable structures. If the growth direction is normal to the plane of the 2D structure then the method can be used to impose minimum member size and to avoid checkerboard problems.

References

[1]Kalpakjian, S. and Schmid, R., "Metal-Casting Processes and Equipment", Manufacturing Engineering and Technology, Fourth Edition. Edited by Prentice Hall.

[2]Bendsoe, M. P. and and Kikuchi, N., "Generating Optimal Topologies in Structural Design Using a Homogenization Method," Comp. Meth. Appl. Mech. Eng., Vol 71, 1988, pp. 197-224.

[3]*GENESIS* User's Manual, Version 7.5, VR&D, Colorado Springs, CO, March 2004.

[4]Harzheim, L. and Graf, G., "TopShape: An attempt to create design proposals including manufacturing constraints," Int. J. Vehicle Design, Vol. 28, No. 4, pp. 389-409, 2002.

[5]Zhou, M., Shyy, Y.K., and Thomas, H.L., "Topology Optimization with Manufacturing Constraints," Proceedings of the 4th World Congress of Structural and Multidisciplinary Optimization, Dalian, China, June 4-8, 2001.

[6]Leiva, J.P., Watson, B.C., and Kosaka, I., "An Analytical Directional Growth Topology Parameterization to Enforce Manufacturing Requirements," Proceedings of the 45th AIAA/ASME/ASCE/AHS/ASC Structures, Structural Dynamics, and Material Conference. Palm Springs, CA, April 19-22,2004.

[7]Schmit, L. A., and Farshi, B., "Some Approximation Concepts for Structural Synthesis," AIAA J., Vol. 12(5), 1974, pp 692-699.

[8]Schmit, L. A., and Miura, H., "Approximation Concepts for Efficient Structural Synthesis," NASA CR-2552, March 1976.

[9]Starnes, J.H. Jr. and Hafka, R.T., "Preliminary Design of Composite Wings for Buckling, Stress and Displacement Constraints," Journal of Aircraft, Vol. 16, Aug. 1979, pp. 564-570.

[10]Fleury, C., and Braibant, V., "Structural Optimization: A new Dual Method using Mixed variables," Int. J. of Numerical Methods in Engineering, Vol. 23, No 3, 1986, pp. 409-429.

[11]Svanberg, K., "The Method of Moving Asymptotes," Int. J. of Numerical Methods in Engineering, Vol. 24, 1987, pp. 359-373.

[12]Salajegheh, E. and Vanderplaats, G. N., "An Efficient Approximation Method for Structural Synthesis with Reference to Space Structures," Space Structures Journal, Vol. 2, No. 3, 1986/87, pp. 165-175.

[13]Vanderplaats, G. N. and Salajegheh, E., "An Efficient Approximation Technique for Frequency Constraints in Frame Optimization," International Journal for Numerical Methods, Vol. 26, 1988, pp 1057-1069.

[14]Yoshida, N. and Vanderplaats, G. N., "Structural Optimization Using Beam Elements," AIAA J., Vol. 26, No. 4, April 1988,pp. 454-462.

[15]Vanderplaats, G. N. and Salajegheh, E., "A New Approximation Method for Stress Constraints in Structural Synthesis," AIAA Journal, Vol. 27, No. 3, March 1989, pp. 352-358.

[16]Canfield, R. A., "High Quality Approximations of Eigenvalues in Structural Optimization of Trusses," AIAA J.,Vol 28, No. 6, 1990, pp. 1116-1122.

[17]Bendsoe, M.P., "Optimal Shape Design as a Material Distribution Problem," Structural Optimization Vol. 1, 1989, pp. 193-202.

[18]Swan, C.C. and Kosaka, I., "Voigt-Reuss topology optimization for structures with linear material behaviors," International Journal for Numerical Methods in Engineering 40: pp. 3785-3814. 1997.

[19]*BIGDOT* User's Manual, Version 2.0, VR&D, Colorado Springs, CO, October 2003.

[20]Leiva, J.P., Watson, B.C., and Kosaka, I., "Modern Structural Optimization Concepts Applied to Topology Optimization," Proceedings of the 40th AIAA/ASME/ASCE/AHS/ASC Structures, Structural Dynamics, and Material Conference. St. Louis, MO, April 12-15,1999, pp. 1589-1596.

[21] T. Belytschko, T., Krongauz,Y., Fleming, M., Organ, D. and Liu, W.K., Smoothing and accelerated computations in the element free Galerkin method," Journal of Computational and Applied Mathematics Volume 74, 111-126 ,1996.

[22]Vanderplaats, G. N. "Very Large Scale Continuous and Discrete Variable Optimization," Proceedings of the 10th AIAA/ISSMO Conference on Multidisciplinary Analysis and Optimization, Albany, New York, Aug 30-Sept.1, 2004.